



*Citation for published version:*

Cabello, G, Gromboni, MF, Pereira, EC & Marken, F 2016, 'In situ microwave-enhanced electrochemical reactions at stainless steel: Nano-iron for aqueous pollutant degradation', *Electrochemistry Communications*, vol. 62, pp. 48-51. <https://doi.org/10.1016/j.elecom.2015.11.007>

*DOI:*

[10.1016/j.elecom.2015.11.007](https://doi.org/10.1016/j.elecom.2015.11.007)

*Publication date:*

2016

*Document Version*

Peer reviewed version

[Link to publication](#)

*Publisher Rights*

CC BY-NC-ND

**University of Bath**

**Alternative formats**

If you require this document in an alternative format, please contact:  
[openaccess@bath.ac.uk](mailto:openaccess@bath.ac.uk)

**General rights**

Copyright and moral rights for the publications made accessible in the public portal are retained by the authors and/or other copyright owners and it is a condition of accessing publications that users recognise and abide by the legal requirements associated with these rights.

**Take down policy**

If you believe that this document breaches copyright please contact us providing details, and we will remove access to the work immediately and investigate your claim.

---

# In situ Microwave-Enhanced Electrochemical Reactions at Stainless Steel: Deposition of Nano-Iron for Aqueous Pollutant Degradation

---

Gema Cabello <sup>a</sup>, Murilo F.Gromboni <sup>a</sup>, Ernesto C. Pereira <sup>a</sup>, Frank Marken <sup>b</sup>

<sup>a</sup> *Department of Chemistry, Universidade Federal de São Carlos, 13565-905 São Carlos, SP, Brazil.*

<sup>b</sup> *Department of Chemistry, Bath University, Bath BA2 7AY, UK.*

## **Abstract**

Iron nanoparticle deposition and stripping are observed from aqueous Fe<sup>2+</sup> solution at pH 3 on stainless electrodes in the presence of focused microwave activation. The effects of Fe<sup>2+</sup> concentration and microwave power (or electrode temperature) are evaluated. It is shown that the resulting iron nanoparticle deposit (i) gives well-defined anodic stripping responses, (ii) is readily released into the solution phase, and (iii) is highly reactive towards chlorinated hydrocarbons such as trichloroacetate. The combined effects of increased mass transport and localised microwave heating are beneficial for pollutant treatment.

## 1. Introduction

Iron nanoparticles are highly reactive and elusive species in aqueous media. The size and properties of iron particles are highly dependent on the preparation conditions and electrochemical reducing methods seem to lead to high purity nanoparticles with a specific size range controlled by the current [1,2,3]. Most work has been focused on the synthesis of iron oxide nanoparticles, but iron nanoparticles are much more reactive and useful, for example as reducing agents or in pollutant treatment.

Direct electrochemical reduction methods have been applied for the degradation of aqueous chloroacetic acids [4-6] (often employed as model chlorinated hydrocarbons), with special attention to the use of iron, or iron modified electrodes. The main source of chloroacetates is the oxidation of chlorine compounds during the disinfection of water supplies. Iron is the main component of pipes for water supply [7] and iron has been extensively used to dehalogenate compounds [8]. A remaining problem is that reductive dehalogenation of chloroacetic acids requires high overpotentials since the reaction takes place at potentials more negative than -1.0 V vs. SCE, concurrently with hydrogen evolution, which diminishes the efficiency of the process [6]. Stainless steel electrodes can be employed in dehalogenation processes as a fairly robust material at negative potentials, resistant to adsorption of impurities, and relatively cheap. Stainless steel has previously been used as cathode material in environmental treatment processes [9,10].

Microwave radiation can be focused into the region close to the electrode surface to give locally enhanced temperatures (with superheating) at the electrode/electrolyte interface [11,12]. A combination of heating (with inverted temperature gradient) and strong mass transport can be

achieved in particular at microelectrodes. In this study, the behaviour of stainless steel electrodes immersed in aqueous solution and with self-focused microwave activation is investigated. It is shown that  $\text{Fe}^{2+}$  in the aqueous solution can lead to well-defined deposition at stripping reactions consistent with the  $\text{Fe}(0)/\text{Fe}(\text{II})$  conversion. Nanoparticle deposits are confirmed by microscopy. The combination is proposed of in situ microwave enhanced formation of iron nanoparticles and the electrocatalytic reduction of chloroacetic acids in aqueous media.

## **2. Experimental Methods**

### ***2.1. Chemicals***

All solutions were prepared using analytical grade reagents (purchased from Aldrich in the purest commercially available grade) and demineralised and filtered water (18.2 M $\Omega$  cm) from an Elgastat water purification system (Elga, Bucks, UK). For microwave experiments solutions were partially degassed using a flow-through vacuum system (ca. 15 Torr achieved with a membrane pump) with electrolyte solution flux of typically 2 mL min<sup>-1</sup>.

### ***2.2. Instrumentation***

Microwave-activated cyclic voltammetry experiments were performed on a Bio-Logic SP-300 electrochemical workstation (Bio-Logic, France). The working electrode was a 50 $\mu\text{m}$ diameter stainless steel wire (AISI 316L) from Advent, embedded in a glass tube with epoxy resin (SP 106, from Gurit). All potentials were measured using a KCl-saturated calomel electrode (SCE) and are reported versus this standard. The auxiliary electrode was a platinum wire. The electrochemical cell (see Figure 1A) was placed inside a modified domestic multimode microwave oven (Panasonic NN-3456) with modified power supply (Oxford Electronics). Details of the cell design and application of microwaves have been described

previously[13]. Scanning electron microscopy (SEM) images were obtained with a JEOL JSM6480LV SEM system.

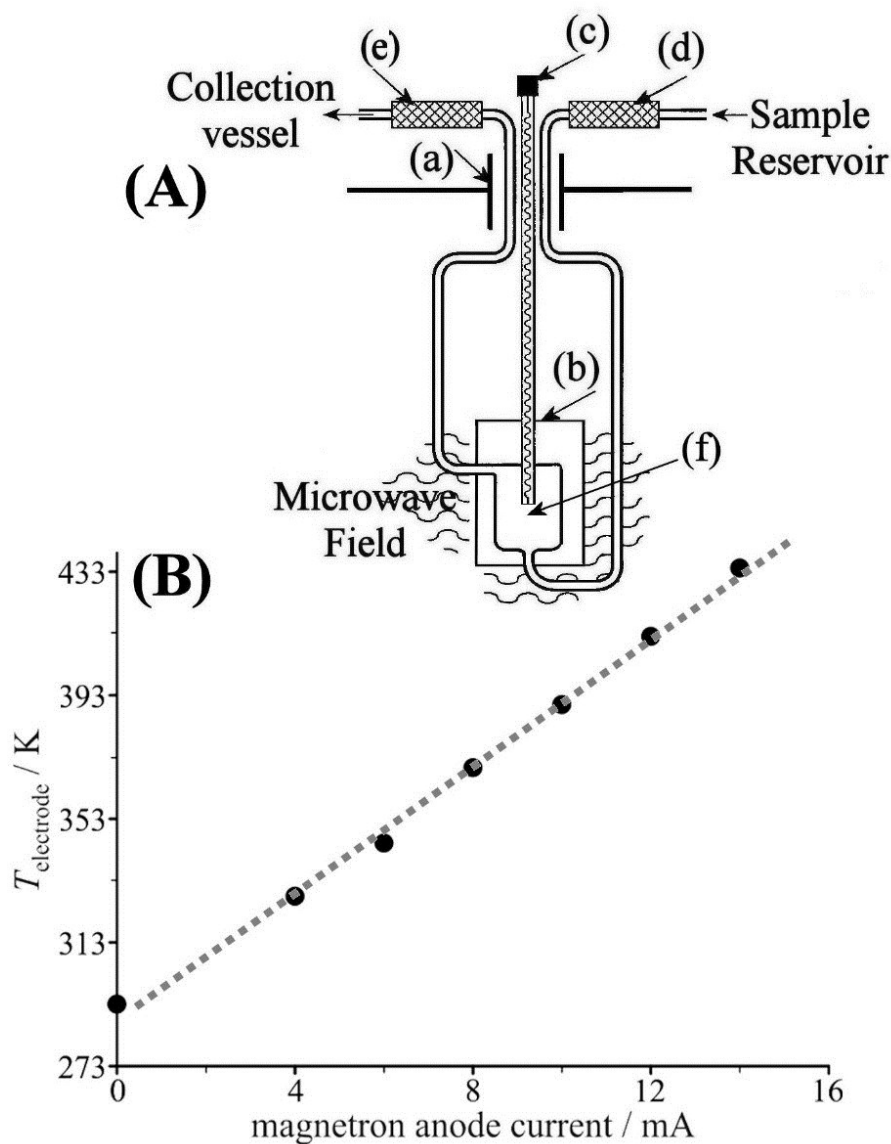


**Figure 1.**(A) Schematic drawing of the flow-through microwave-electrochemical cell with (a) the cavity port, (b) a Teflon cell, (c) a stainless steel microelectrode as working electrode, (d) the reference electrode, (e) the counter electrode, and (f) the location where microwave energy is focused. (B) Plot of the variation of the temperature of a 50 μm stainless steel electrode as a function of the applied microwave intensity (magnetron anode current), calculated from the equilibrium potential of 10 mM Fe(CN)<sub>6</sub><sup>3-</sup> / 10 mM Fe(CN)<sub>6</sub><sup>4-</sup> in 1 M KCl (see text).

### 3. Results and Discussion

#### 3.1. Microwave Effects on Electrochemical Processes at Stainless Steel I.: $\text{Fe}(\text{CN})_6^{3-}/\text{Fe}(\text{CN})_6^{4-}$ Calibration

Electrochemical processes in the presence of self-focused microwave radiation experience both faster mass transport and elevated temperatures. Therefore, a temperature calibration is required, since the operating temperature is controlled by changing the anode current of the microwave magnetron. It is well known [13] that the  $\text{Fe}(\text{CN})_6^{3-}/4-$  redox system is a suitable system for quantifying the effect of thermal activation, since an increase of the temperature at the electrode surface will provoke a linear shift of the equilibrium potential, due to the reaction entropy associated with the redox process[14]. The shift in the equilibrium potential for a solution containing 10 mM  $\text{Fe}(\text{CN})_6^{4-}$  and 10 mM  $\text{Fe}(\text{CN})_6^{3-}$  in 1 M KCl, recorded with microwave pulses and under non-isothermal heating conditions, with an electrolyte flow rate of 2 mL min<sup>-1</sup>, as a function of the temperature can be assumed to follow  $dE_{\text{equilibrium}}/dT = -1.7 \pm 0.05 \text{ mV k}^{-1}$  [15]. Figure 1B shows the temperature data (the local electrode temperature which may be lower than the adjacent solution temperature) as a function of the applied microwave power (expressed as magnetron current). As expected, the equilibrium potential shifts to more negative potentials in the presence of microwave radiation and similar temperatures are obtained here at stainless steel compared to those reported in previous works for other types of electrodes [15].

#### 3.2. Microwave Effects on Electrochemical Processes at Stainless Steel II.: Reduction of Aqueous $\text{Fe}^{2+}$

Self-focused microwave radiation has been previously proven to be suitable to enhance electrochemical processes such as deposition and stripping detection of heavy metals [16,17]

and, typically, platinum, gold, and glassy carbon electrodes have been employed [18,19]. There are no previous records of the direct application of self-focused microwave radiation at stainless steel electrodes and for the electrosynthesis of metal nanoparticles.

Aqueous  $\text{Fe}^{2+}$  can be easily reduced to  $\text{Fe}^0$  at the surface of a stainless steel microelectrode under microwave conditions and from a solution of 1 mM  $\text{Fe}^{2+}$  at pH 3, as shown in the scanning electron microscopy images (see Figure 2). Figure 2a shows the featureless polished stainless steel surface; Figure 2b shows the surface of the steel electrode after exposure to microwave radiation for 5 minutes (10 mA magnetron current) in a solution containing 0.1 M  $\text{Na}_2\text{SO}_4$  (pH 3). It can be observed that the epoxy resin around the steel wire has been damaged by the action of the heat, causing some resin melting/leaching or swelling to partially cover the electrode surface. Figure 2c and d show the surface after  $\text{Fe}^0$  nanoparticle deposition (probably in the form of iron oxide after exposure to air). It can be inferred that  $\text{Fe}^0$  nanoparticles have been formed at the electrode surface and that, due to the high electrolyte flow, they have been dislodged or expelled from the surface towards the edge between the electrode and the resin that is porous (Figure 2b) probably due to the high temperatures reached at the vicinity of the electrode surface. Consequently, the electrode surface seems to be continuously generating  $\text{Fe}^0$  nanoparticles (see below).

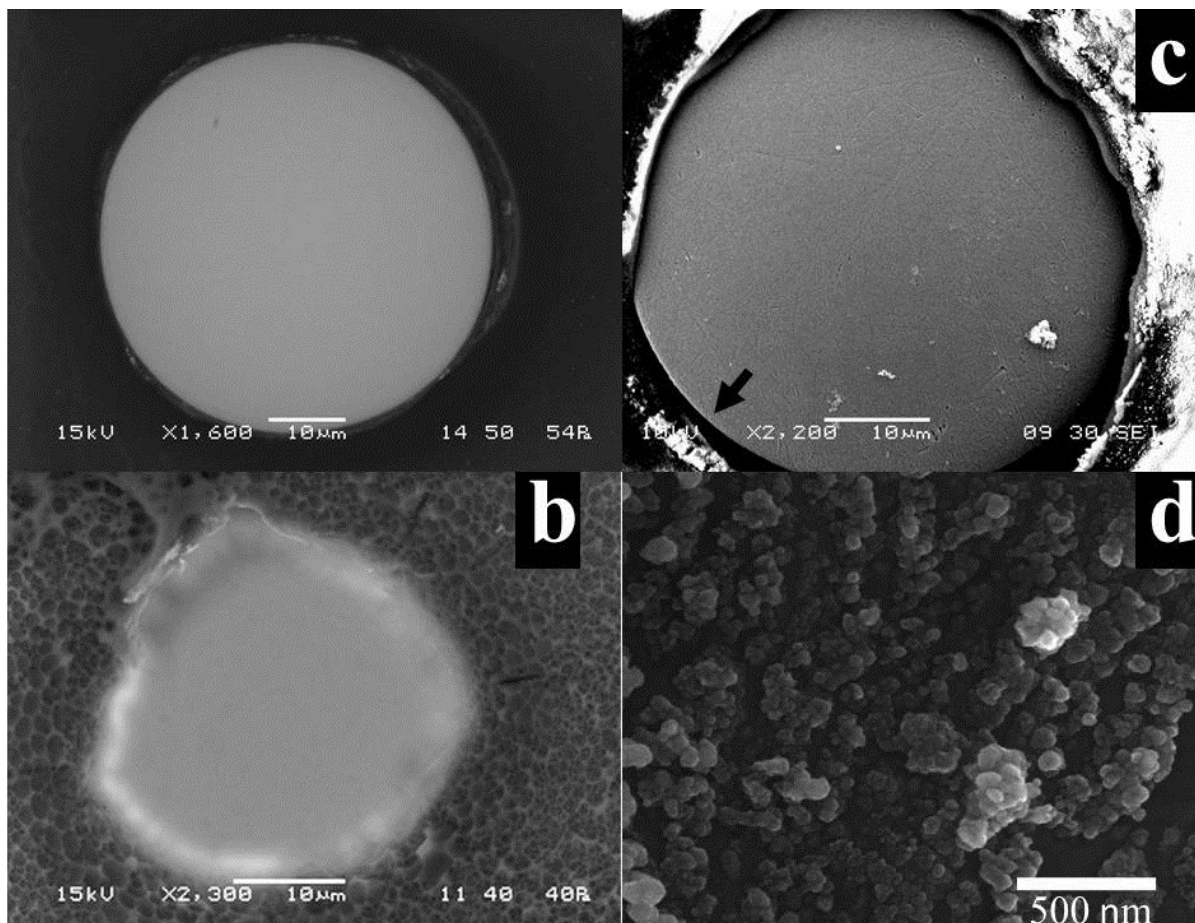


**Figure 2.** SEM images showing the surface of a 50  $\mu\text{m}$  stainless steel electrode. (a) Polished surface; (b) after microwave radiation exposure (10 mA magnetron current, 5 min) in a solution containing 0.1 M  $\text{Na}_2\text{SO}_4$  (pH 3); (c) after microwave radiation exposure (10 mA magnetron current, 1 min) in a solution containing 1 mM  $\text{FeSO}_4$  in 0.1 M  $\text{Na}_2\text{SO}_4$  (pH 3).

Iron deposition onto the stainless steel surface was characterized voltammetrically by studying the evolution of the iron stripping peak under different working conditions, i.e.  $\text{Fe}^{2+}$  concentration, temperature and deposition time. Iron deposition and re-dissolution occurs effectively under microwave radiation, and the effect of the iron concentration on the  $\text{Fe}^0$  formation at the steel microelectrode was evaluated studying the stripping peak. Figure 3A shows cyclic voltammograms obtained for solutions of  $\text{FeSO}_4$  with different concentrations. The iron stripping peak is absent when a solution containing just 0.1 M  $\text{Na}_2\text{SO}_4$  is used (Fig 3A-a). On the other hand, in solutions containing  $\text{Fe}^{2+}$  from 0.5 mM to 4mM the stripping response for the iron re-dissolution is clearly observed. The stripping response starts at around

-0.8 V and it can be observed that the stripping peak markedly increases with the  $\text{Fe}^{2+}$  concentration (0.5 mM  $\text{Fe}^{2+}$  being the lower limit concentration for the formation of  $\text{Fe}^0$  under microwave constant power of 8 mA) (Figure 3A: b-e). Peaks become narrower and more intense as the concentration increases until 4 mM  $\text{Fe}^{2+}$  and there is a clear shift in the peak position for the stripping process. However, peaks broaden at higher concentrations (data not shown). Reduction currents increase with increasing the  $\text{Fe}^{2+}$  concentration as well, leading to sigmoidal cathodic currents typical of enhanced mass processes.

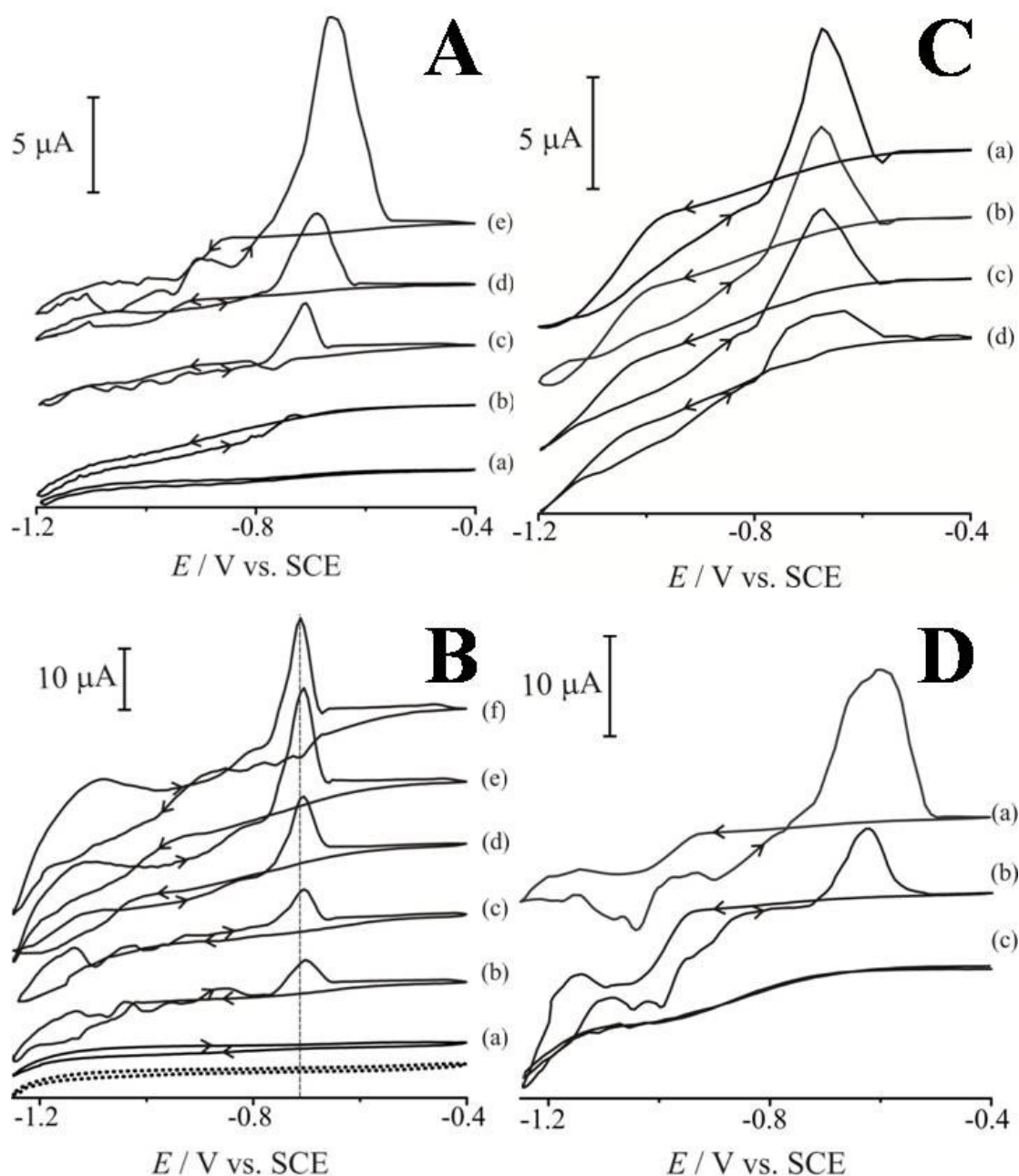


**Figure 3.** Cyclic voltammograms for the reduction and stripping of  $\text{Fe}^{2+}$ , at a  $50 \mu\text{m}$  diameter steel electrode (A) at  $20 \text{ mV s}^{-1}$ , in a solution containing (a)  $0.0 \text{ mM}$ , (b)  $0.5 \text{ mM}$ ; (c)  $1 \text{ mM}$ ; (d)  $2 \text{ mM}$ ; (e)  $4 \text{ mM}$   $\text{FeSO}_4$  in  $0.1 \text{ M}$   $\text{Na}_2\text{SO}_4$  ( $\text{pH } 3$ ),  $8 \text{ mA}$  microwave magnetron current. In a solution containing  $1 \text{ mM}$   $\text{FeSO}_4$  in  $0.1 \text{ M}$   $\text{Na}_2\text{SO}_4$  ( $\text{pH } 3$ ): (B) Without (dotted line) and with (continuous line) microwave radiation, applying a magnetron current of (a)  $6 \text{ mA}$ ; (b)  $8 \text{ mA}$ ; (c)  $10 \text{ mA}$ ; (d)  $12 \text{ mA}$ ; (e)  $14 \text{ mA}$ ; (f)  $16 \text{ mA}$ , at  $20 \text{ mV s}^{-1}$  and (C) At a scan rate of  $10 \text{ mV s}^{-1}$  (a);  $20 \text{ mV s}^{-1}$  (b);  $50 \text{ mV s}^{-1}$  (c); and  $100 \text{ mV s}^{-1}$  (d),  $10 \text{ mA}$  microwave magnetron current. (D) At a scan rate of  $20 \text{ mV s}^{-1}$  in a solution containing (a)  $4 \text{ mM}$   $\text{FeSO}_4$  in  $0.1 \text{ M}$   $\text{Na}_2\text{SO}_4$ ; (b)  $4 \text{ mM}$  TCAA and  $4 \text{ mM}$   $\text{FeSO}_4$  in  $0.1 \text{ M}$   $\text{Na}_2\text{SO}_4$ ; (c)  $4 \text{ mM}$  TCAA in  $0.1 \text{ M}$   $\text{Na}_2\text{SO}_4$  (all  $\text{pH } 3$ ),  $7 \text{ mA}$  microwave magnetron current.

The influence of the temperature, measured as the magnetron anode current, in the iron deposition can be characterized by the iron stripping peak (Figure 3B). The reductive-deposition of iron at steel electrodes is a process that necessarily requires high temperatures, as shown by the absence of the stripping peak when no microwave radiation is applied (Figure 3B, dotted line) or under microwave conditions but at low temperatures (Figure 3B-a, 6 mA magnetron current, corresponding to ca. 343 K). At higher temperatures, the stripping peaks are better defined and become narrower, since higher microwave radiation levels enhance the iron dissolution process and higher stripping peaks are recorded, until the limit higher temperature (at which the iron stripping peak no further changes) is reached, when 16 mA magnetron currents are applied and corresponding to ca. 440 K (Figure 3B-f). Higher microwave power provokes an increase in the limiting current, attributed to the generation of a high-temperature region at the electrode/electrolyte interface [12]. Accordingly, the shape of the voltammograms changes from the conventional peak-shaped characteristic of room temperature (Figure 4, dotted line), into sigmoidal (Figure 3B: a-f), indicating an increase in the mass transport as a consequence of convection processes [20]. The direct/additional heating effects induced by microwave adsorption into the metallic iron nanoparticles may also play a role, but experimental evidence for this is currently not available.

To study the effect of the deposition time on the stripping peak, cyclic voltammetry experiments were performed at different scan rates: 10, 20, 50 and 100 mV s<sup>-1</sup> (Figure 3C). The reduction of Fe<sup>2+</sup> starts at -0.5 V and the reduction signal, attributed to Fe<sup>0</sup> nucleation, can be observed until -1.2 V where the hydrogen evolution starts taking place. In the positive-going sweep, the characteristic peak of the iron stripping can be observed, and a systematic decrease in the peak area occurs as the scan rate increases. Iron reduction has been performed only during the cathodic sweep (no further deposition potential has been applied). Consequently, improved

stripping peaks are detected as the scan rate is slower. Reduction currents increase with increasing the  $\text{Fe}^{2+}$  concentration as well, leading to the same sigmoidal cathodic currents typical of enhanced mass processes, in concordance with the data obtained in Figure 3A.

### 3.3. Microwave Effects on Electrochemical Processes at Stainless Steel III.: Reduction of Chloroacetates

Dehalogenation processes of organic contaminants in water using, mainly, iron in its zero oxidation state have extensively been studied for decades due to its reducing character [7] (equation 1).



Here RX represents a halogenated hydrocarbon and  $\text{X}^-$  is the corresponding halide. It has been previously shown that this reaction follows the reductive sequence of tri-, di- and mono-chloroacetic acid, until acetic acid is formed as the final product [21]. In order to characterize the iron-modified steel electrode for use in cathodic electrode processes, the reduction of trichloroacetic acid (TCCA) has been studied.

Figure 3D shows the cyclic voltammograms for the iron reduction and stripping in a solution containing 4 mM  $\text{FeSO}_4$  (Figure 3D-a); containing 4 mM  $\text{FeSO}_4$  and 4 mM TCCA (Figure 3D-b); and for the TCCA reduction of a solution containing 4 mM TCAA, all in 0.1 M  $\text{Na}_2\text{SO}_4$ , pH 3 (Figure 3D-c). The reduction process of trichloroacetic acid starts at -0.8 V (Figure 3D-c) coinciding with the potential of iron deposition. The highest reduction current observed when

both,  $\text{Fe}^{2+}$  and TCAA, are present in the solution, together with the ca. 3-fold decrease in the iron stripping peak area, compare to the solution in the absence of TCAA, suggest that the TCAA reduction is taking place (competitively with iron deposition) and the process is enhanced by microwaves and the higher concentration of  $\text{Fe}^0$  at the electrode surface at more negative potentials. These are preliminary results and further study of the optimisation of the process and effects of microwaves on the chemical process are required.

#### **4. Conclusion**

Iron nanoparticles obtained by microwave-activated electro-reduction onto a stainless steel microelectrode have been studied for the degradation of trichloroacetic acid in aqueous solution. Preliminary results show that microwave radiation provides a beneficial reaction environment for the reduction reaction of  $\text{Fe(II)}$  to iron to take place at the steel electrode surface, with promising applications in the cathodic dehalogenation of chloroacetic acids. The method could be useful for a wider range of processes based on highly reactive iron nanoparticles.

#### **Acknowledgements**

CNPq is gratefully acknowledged for financial support under Research Project BJT-2014/400117/2014-2.

#### **References**

- [1] Zoval, J.V., Stiger, R.M., Biernacki, P.R., Penner, R.M. *The Journal of Physical Chemistry* (1996), 100, 2, 837-844.

- [2] Rodríguez-Sánchez, L., Blanco, M.C., López-Quintela, M.A. *The Journal of Physical Chemistry B* (2000), 104, 41, 9683-9688.
- [3] Welch, C., Compton, R. *Anal Bioanal Chem* (2006), 384, 3, 601-619.
- [4] Kvaratskheliya, R.K., Kvaratskheliya, E.R. *Russ. J. Electrochem.* (2001), 37, 9, 968-971.
- [5] Korshin, G.V., Jensen, M.D. *Electrochim. Acta* (2001), 47, 5, 747-751.
- [6] Altamar, L., Fernández, L., Borrás, C., Mostany, J., Carrero, H., Scharifker, B. *Sens. Actuators, B* (2010), 146, 1, 103-110.
- [7] Hozalski, R.M., Zhang, L., Arnold, W.A. *Environmental Science & Technology* (2001), 35, 11, 2258-2263.
- [8] Eggen, T., Majcherczyk, A. *Chemosphere* (2006), 62, 7, 1116-1125.
- [9] Nylén, L., Cornell, A. *J. Appl. Electrochem.* (2009), 39, 1, 71-81.
- [10] Esclapez, M.D., Díez-García, M.I., Sáez, V., Bonete, P., González-García, J. *Environ. Technol.* (2012), 34, 3, 383-393.
- [11] G. Compton, R., A. Coles, B., Marken, F. *Chem. Commun.* (1998), 23, 2595-2596.
- [12] Marken, F., Tsai, Y.-C., Coles, B.A., Matthews, S.L., Compton, R.G. *New Journal of Chemistry* (2000), 24, 9, 653-658.
- [13] Marken, F., Matthews, S.L., Compton, R.G., Coles, B.A. *Electroanalysis* (2000), 12, 4, 267-273.
- [14] Turner, J.W., Schultz, F.A. *Inorganic Chemistry* (1999), 38, 2, 358-364.
- [15] Rassaei, L., French, R.W., Compton, R.G., Marken, F. *Analyst* (2009), 134, 5, 887-892.
- [16] Tsai, Y.-C., Coles, B.A., Compton, R.G., Marken, F. *Electroanalysis* (2001), 13, 8-9, 639-645.

- [17] Tsai, Y.-C., Coles, B.A., Holt, K., Foord, J.S., Marken, F., Compton, R.G. *Electroanalysis* (2001), 13, 10, 831-835.
- [18] Cutress, I.J., Marken, F., Compton, R.G. *Electroanalysis* (2009), 21, 2, 113-123.
- [19] Marken, F. *Annual Reports Section "C" (Physical Chemistry)* (2008), 104, 0, 124-141.
- [20] Tsai, Y.-C., Coles, B.A., Compton, R.G., Marken, F. *Journal of the American Chemical Society* (2002), 124, 33, 9784-9788.
- [21] Li, X.-Q., Zhang, W.-X. *Langmuir* (2006), 22, 10, 4638-4642.